

# Structural Evolution of Ga–Cu Model Catalysts for CO<sub>2</sub> Hydrogenation Reactions

Jian-Qiang Zhong, Shamil Shaikhutdinov,\* and Beatriz Roldan Cuenya



Cite This: *J. Phys. Chem. C* 2021, 125, 1361–1367



Read Online

ACCESS |



Metrics & More

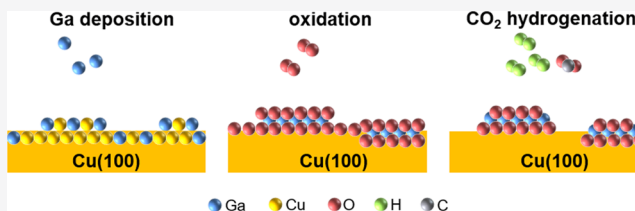


Article Recommendations



Supporting Information

**ABSTRACT:** We studied the initial stages of Ga interaction with the Cu(001) surface and environment-induced surface transformations in an attempt to elucidate the surface chemistry of the Cu–Ga catalysts recently proposed for CO<sub>2</sub> hydrogenation to methanol. The results show that Ga readily intermixes with Cu upon deposition in vacuum. However, even traces of oxygen in the gas ambient cause Ga oxidation and the formation of two-dimensional (“monolayer”) Ga oxide islands uniformly covering the Cu surface. The surface morphology and the oxidized state of Ga remain in H<sub>2</sub> as well as in a CO<sub>2</sub> + H<sub>2</sub> reaction mixture at elevated pressures and temperatures (0.2 mbar, 700 K). The results indicate that the Ga-doped Cu surface under reaction conditions exposes a variety of structures including GaO<sub>x</sub>/Cu interfacial sites, which must be taken into account for elucidating the reaction mechanism.



## 1. INTRODUCTION

Gallium-containing alloys and intermetallic compounds have recently received significant attention in catalysis, in particular, for industrially important processes such as selective hydrogenation of alkynes (on Pd–Ga)<sup>1</sup> and CO<sub>2</sub> hydrogenation to methanol (on Ni–Ga).<sup>2,3</sup> The methanol synthesis was found to proceed with relatively high activity and selectivity on Ni<sub>3</sub>Ga<sub>3</sub>/SiO<sub>2</sub> catalysts even at an ambient pressure. The latter is important for the development of small-scale devices operating at low pressures using solar-generated hydrogen. On the basis of theoretical considerations, the reactivity has been attributed to the formation of Ga-rich metallic sites.<sup>2</sup> On the other hand, Ga is prone to oxidation,<sup>4</sup> thus resulting in a Ga oxide shell, surrounding a metallic core of nanoparticles (NPs),<sup>5</sup> which can only be reduced in hydrogen at high temperatures.

The discovery of the Ni–Ga catalysts triggered studies on other Ga-promoted 3d metal catalysts, in particular, Cu,<sup>6</sup> which is a crucial component of the industrial Cu/ZnO/Al<sub>2</sub>O<sub>3</sub> catalyst for methanol production. A strong promotional effect of Ga was observed on SiO<sub>2</sub>-supported Cu NPs. The addition of Ga increased the methanol formation rate without a significant change in the reverse water–gas shift reaction. The results suggested that Ga promotes Cu by increasing its methanol selectivity, likely by creating new active sites for methanol formation without modifying its oxidation state, which remains mostly metallic under the reaction conditions. However, the formation of a Ga<sub>2</sub>O<sub>3</sub> phase that activates CO<sub>2</sub> has been used to explain the infrared spectra.<sup>6</sup> Nevertheless, surface structures and surface reactions on Ni–Ga and Cu–Ga nanoparticulate systems remain far from being well understood. In this respect, “surface science” studies employing

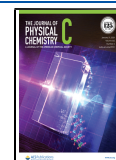
surface-sensitive techniques applied to well-defined model systems may provide substantial insights into atomic structures and the surface chemistry of the Ga-based catalysts and aid in understanding the promotional effects of Ga in hydrogenation reactions.

To date, most of the model studies performed on Ga–3d metal compounds were primarily focused on the growth of Ga oxide thin films because of its application in various disciplines related to microelectronics, solar cells, and gas sensors.<sup>7</sup> Upon exposure to oxygen at 300 K, an amorphous Ga oxide thin film forms on the CoGa(110) and CoGa(001) surfaces. At high temperatures (above 700 K), it transforms into an ordered structure assigned to a thin film of β-Ga<sub>2</sub>O<sub>3</sub>.<sup>8,9</sup> A more recent in situ surface X-ray diffraction study<sup>10</sup> of CoGa(001) complemented with density functional theory calculations revealed that the ultrathin oxide film consists of an oxygen ion double layer containing the basic building block of β-Ga<sub>2</sub>O<sub>3</sub>. Ultrathin films of Ga<sub>2</sub>O<sub>3</sub> were also grown on a Ni(100) substrate by oxidation of a ~15 Å-thick Ga film prepared by physical vapor deposition.<sup>11,12</sup> Upon O<sub>2</sub> exposure at room temperature, an amorphous Ga oxide layer formed on top of the metallic Ga layer. Subsequent annealing at 700 K in vacuum led to the formation of a well-ordered oxide film tentatively assigned to the γ'-Ga<sub>2</sub>O<sub>3</sub> phase exposing the (111)

**Received:** October 16, 2020

**Revised:** November 30, 2020

**Published:** January 6, 2021



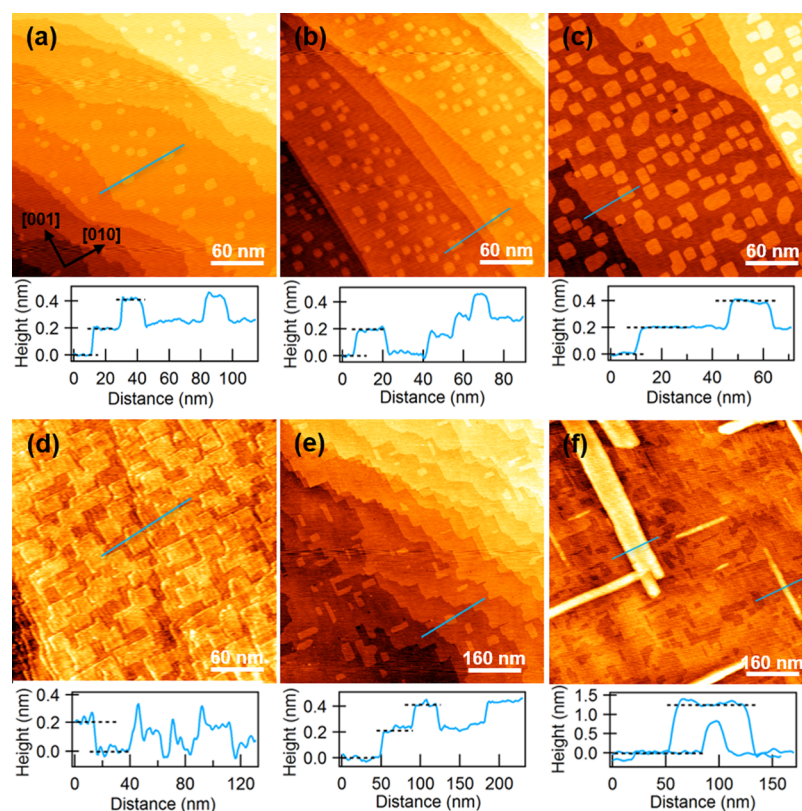


**Figure 1.** STM images of Ga deposited on Cu(001) at 300 K at increasing deposition time (a–f). The height profiles along the lines are shown below the images. Tunneling parameters (bias and current) are (a) 0.5 V, 0.05 nA, (b) 1.5 V, 0.08 nA, (c) 0.3 V, 0.05 nA, (d) 1.0 V, 0.2 nA, (e) 0.7 V, 0.2 nA, and (f) 0.38 V, 0.29 nA.

surface.<sup>11</sup> Interestingly, the diffraction pattern observed on this film is very similar to that reported for a Ga oxide film formed on the CoGa(110) surface,<sup>8</sup> pointing to the similar structural motif of the Ga oxide films on both metal surfaces.

To the best of our knowledge, such studies are missing for the Ga–Cu system. Actually, the interest in the Ga–Cu interaction is still largely driven by the use of liquid Ga-based alloys in low-temperature soldering in microelectronics.<sup>13</sup> The Ga–Cu equilibrium phase diagram is quite complex. At least 10 different phases were found.<sup>14</sup> Among those, the CuGa<sub>2</sub> intermetallic phase is the dominant phase formed at Ga/Cu interfaces at room temperature, which induces the wetting behavior of liquid Ga via stable metallic bonds to Cu.<sup>15</sup> Note also that this phase is the most stable at relatively low temperatures (below 550 K), a typical temperature range of the CO<sub>2</sub> hydrogenation reaction.

In order to get more insights into the Ga–Cu interaction, in particular, the Ga–Cu surfaces and their transformations under catalytically relevant conditions, here we prepared planar model systems by physical vapor deposition of Ga onto a Cu(001) substrate. The surface structures were studied by low-energy electron diffraction (LEED), Auger electron spectroscopy (AES), scanning tunneling microscopy (STM), temperature-programmed desorption (TPD), and near-ambient pressure X-ray photoelectron spectroscopy (NAP–XPS). The results suggest that metallic Ga readily intermixes with the Cu surface upon deposition. However, even traces of oxygen in the gas ambient cause oxidation of Ga and the formation of two-dimensional Ga oxide nanoislands uniformly covering the Cu surface. The morphology and the oxidized state of Ga remain in a pure H<sub>2</sub> atmosphere as well as in the CO<sub>2</sub> + H<sub>2</sub> reaction

mixture. Obviously, the Ga-doped Cu surface under CO<sub>2</sub> hydrogenation reaction conditions exposes a variety of surface structures, particularly GaO<sub>x</sub>/Cu interfacial sites, which have to be taken into account for elucidating the reaction mechanism.

## 2. METHODS AND MATERIALS

The experiments were carried out in an ultrahigh vacuum (UHV) chamber equipped with LEED/AES (from Specs), STM (Omicron), and a quadrupole mass spectrometer (QMS, from Hiden). The Cu(001) single crystal (MaTeck GmbH) was mounted onto a sample holder plate having a hole to ease sample heating by electron bombardment from the backside of the crystal using a tungsten filament. The temperature was measured using a chromel–alumel thermocouple clamped at the edge of the Cu crystal. The surface was cleaned by several cycles of Ar<sup>+</sup> sputtering and UHV annealing at 800 K, until the LEED shows sharp diffraction spots and no impurities were detected by AES. Gallium (Aldrich, 99.999%) was deposited using an electron-beam assisted evaporator (Focus EFM3) from a BN crucible placed in a Mo liner. All STM images were obtained in vacuum at room temperature using Pt–Ir tips.

NAP–XPS measurements were performed in another UHV chamber (Specs) equipped with a monochromatic Al K $\alpha$  X-ray source ( $h\nu = 1486.6$  eV) and a hemispherical analyzer (Phoibos 150 NAP). The samples were transferred between the two UHV setups using a vacuum suitcase having a background pressure below 10<sup>−7</sup> mbar.

## 3. RESULTS AND DISCUSSION

Figure 1 shows the STM images obtained on the Cu(001) surface after Ga deposition at room temperature as a function

of the deposition time. Note that a clean Cu substrate was prepared prior to each deposition. At low Ga coverages, that is, when the ratio of the Ga (at 1070 eV) and Cu (at 921 eV) peaks in AES spectra (see Figure S1 in the Supporting Information) is below 0.1, the STM images revealed square-shaped islands randomly distributed on the terraces (Figure 1a–c). Interestingly, there is no preferential nucleation at step edges. The island density (Figure 1a,b) and then the island size (Figure 1b–d) both increase with the increasing deposition time, indicating that the islands are pure Ga in nature. Accordingly, the square shape of the islands points to the formation of an epitaxial Ga(001) layer. The height of the islands is virtually identical to that measured for the monolayer steps separating the Cu(001) terraces. The latter can, in principle, be explained by the atomic radius of metallic Ga being only slightly smaller than that of Cu (130 and 135 pm, respectively), thus making them hardly distinguishable in the topographic STM images. On further increasing the coverage (Figure 1e), the islands coalesce and the surface becomes uniformly covered with a few similarly oriented rectangular islands. The latter seem to be the precursors for the formation of much larger structures imaged like flat-lying “sticks” several hundreds of nanometers long and only about 1.5 nm high (Figure 1f). Based solely on the STM images, one can tentatively conclude that Ga grows on the Cu(001) surface in the Stranski–Krastanov mode, that is, first forming an epitaxial Ga layer on top of which three-dimensional structures start to grow at further Ga deposition.

To shed more light on the atomic structure of the Ga/Cu(001) surface, we studied the adsorption of CO as a probe molecule, commonly used for mono- and bimetallic surfaces.<sup>16,17</sup> Figure 2a shows the TPD spectra obtained on

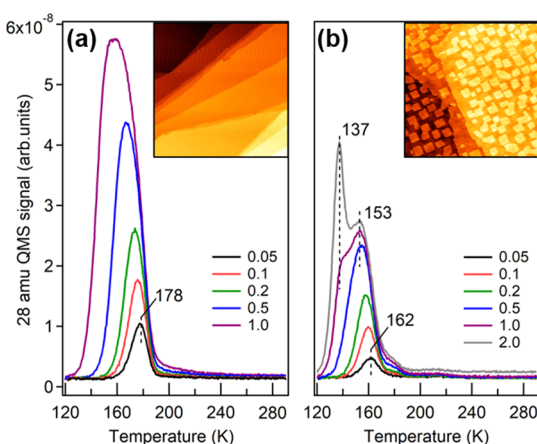


**Figure 2.** TPD spectra of CO adsorbed at 130 K on a clean Cu(100) surface (a) and a Ga/Cu(100) surface (b) at CO exposures (in L) as indicated. The heating rate was 2 K/s. The inset shows STM images (300 nm  $\times$  300 nm) of the samples studied.

the clean Cu(001) surface as a function of CO exposure (in Langmuir (L), 1 L =  $10^{-6}$  Torr  $\times$  s). One desorption peak is observed that gains in intensity and shifts to lower temperatures with increasing CO dosage.

The spectra changed considerably after Ga deposition (Figure 2b). Based on the STM images (see the inset in Figure 2b and also Figure 1c), and assuming that all deposited Ga atoms form Ga(001) monolayer islands, Ga covers about 50% of the Cu surface in this sample. Therefore, one

anticipates the desorption signal from uncovered Cu(001) to be attenuated by a factor of two. Accordingly, all other signals should be associated with CO adsorption on the Ga(001) surface. However, the spectra showed a different picture (Figure 2b). At the lowest CO exposure, the peak appears at 162 K, which is 16 K lower than that for the clean Cu(001) surface at the same dosage. With the increasing CO exposure, this signal gains in intensity, shifts to a lower temperature, and saturates at about 1 L. Concomitantly, a new feature shows up at 137 K at higher dosages, and a weak signal appears at around 180 K. It may well be, however, that the former one solely represents a “cut-off tail” of CO desorption having a maximum at the lower temperature.

Therefore, in contrast to the STM-based model of Ga(001) islands surrounded by pristine Cu(001), the TPD results point to the absence of a pure Cu(001) surface. Apparently, the Ga adatoms intermix with the Cu surface at room temperature, probably in the same manner as observed for Zn–Cu systems (ref.<sup>18</sup> and the references therein). The conclusion is further supported by STM results on the samples exposed to oxygen.

Figure 3 shows the room-temperature STM images of the Ga/Cu(001) surface after annealing in UHV and then in  $10^{-7}$  mbar of O<sub>2</sub> at several different temperatures as indicated. Clearly, the islands become larger at 400 K (Figure 3a,b), probably via an Ostwald ripening mechanism, which, in turn, implies the high diffusivity of surface atoms.<sup>19</sup> The morphology does not change much after exposure to oxygen at 400 K. The surface reconstructs and becomes considerably rougher at 500 K and remains as such after annealing at higher oxidation temperatures (600–700 K). However, the islands and the terraces show a virtually identical morphology. This finding points to a uniform distribution of Ga in the initial sample, both within islands and on terraces, in full agreement with the above-presented TPD results showing the absence of CO desorption signals of pure Cu(001).

To get information about the chemical states of Cu and Ga, we employed XPS. The “as-deposited” Ga/Cu(001) samples were transferred to another UHV setup using a vacuum suitcase (base pressure <  $10^{-7}$  mbar). Figure 4 shows the XPS spectra of the Ga 2p<sub>3/2</sub>, Cu 2p<sub>3/2</sub>, and O 1s core levels as well as the Cu LMM Auger transition region that allows to distinguish Cu(I) and Cu(0) species. The Cu 2p<sub>3/2</sub> peak at 932.5 eV in combination with the Auger line at 568.1 eV are fingerprints of metallic Cu, expected for the “as-deposited” Ga/Cu(001) surface. A small O 1s signal detected at 530.7 eV (Figure 4b) suggests that Ga deposits are partially oxidized during sample transfer due to the well-known high affinity of Ga to oxygen. Indeed, a prominent shoulder appears in the Ga 2p<sub>3/2</sub> region at 1117.5 eV in addition to the main peak at 1116.4 eV (Figure 4a) corresponding to oxidized and metallic Ga, respectively.<sup>4,20</sup> After exposure to  $10^{-7}$  mbar of O<sub>2</sub> at 400 K, the 1117.5 eV signal gains in intensity, while the 1116.4 eV signal attenuates. The oxidation seems to be completed at 500 K as no more changes are detected after exposure at 600 and 700 K, in agreement with the STM results showing no further morphological changes (see Figure 3). However, during these surface transformations, Cu remains metallic (Figure 4b,c) although the presence of O atoms on Cu(001) cannot be excluded. Indeed, in addition to the main peak at 530.7 eV associated with the Ga oxide phase, there is a weak signal at 529.8 eV, which was observed on the Ga-free Cu(001) surface (Figure S2 in the Supporting Information). Another weak state at 532.3 eV is tentatively assigned to traces of carbonates



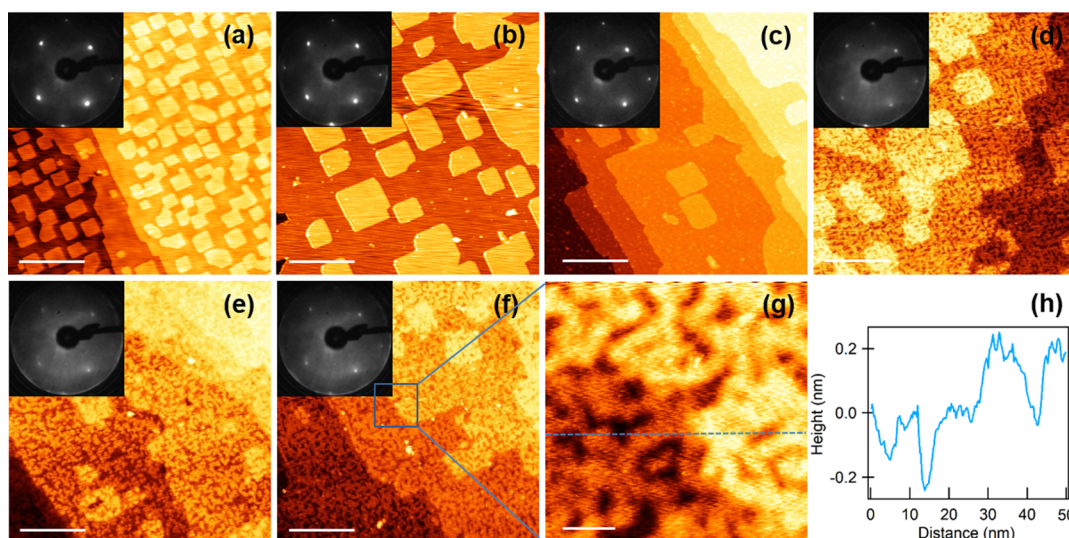


**Figure 3.** Room-temperature STM images of Ga on Cu(100) as-deposited (a), after annealing first in UHV at 400 K (b), and then in  $1 \times 10^{-7}$  mbar of  $O_2$  at 400 K (c), 500 K (d), 600 K (e), and 700 K (f) for 5 min each. (g) The zoomed-in image of (f). (h) Topography profile along the dashed line indicated in (g). The scale bar in (a–f) is 75 nm and that in (g) is 10 nm. The corresponding LEED patterns (at 123 eV) are shown as insets. Tunneling parameters (bias and current) are (a) 1.0 V, 0.2 nA, (b) 1.0 V, 0.2 nA, (c) 1.0 V, 0.1 nA, (d)  $-0.5$  V, 0.06 nA, (e) 0.5 V, 0.05 nA, (f) 1.0 V, 0.05 nA, and (g) 0.5 V, 0.1 nA.

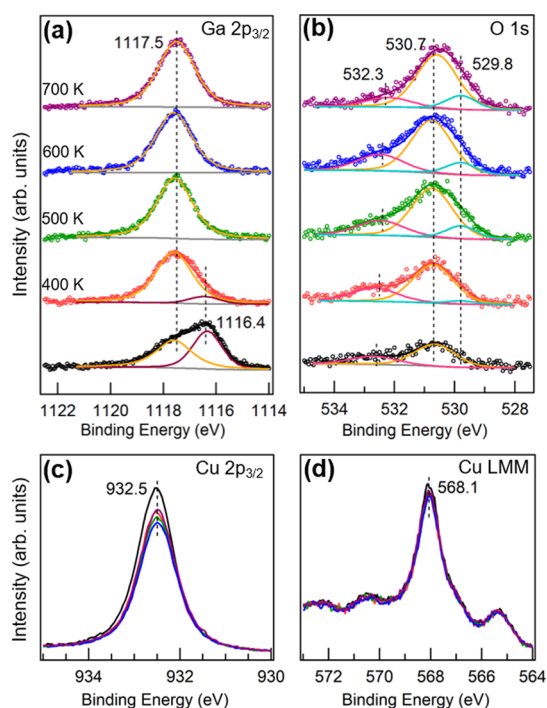


**Figure 4.** XPS spectra of the Ga/Cu(100) surface measured at 300 K in UHV before (black) and after annealing in  $1 \times 10^{-7}$  mbar of  $O_2$  at 400, 500, 600, and 700 K as indicated in the same color code in all panels. In addition to the Ga 2p, O 1s, and Cu 2p core level regions, the Cu LMM Auger lines are also shown. The typical morphology of the sample before the XPS measurements is shown in Figure 3a.

( $CO_3^{2-}$ ) (see also Figure S3 for the C1s region) and/or hydroxyls (OH) caused by the reaction of Ga oxide with residual  $CO_2$  and water molecules in the vacuum background.

Therefore, the combined STM and XPS results clearly show an oxygen-induced phase separation of the initially bimetallic Ga–Cu surface into a Ga oxide and a pure Cu surface, ultimately resulting in surface roughening (Figure 3). It is

interesting to note that the corrugation amplitude measured on oxidized samples by STM (Figure 3h) is close to or slightly below the monoatomic step height of a substrate, suggesting that either Ga oxide forms an ultrathin film or the image contrast is actually dominated by an electronic rather than a topographic contribution. Figure 5 shows the STM images of

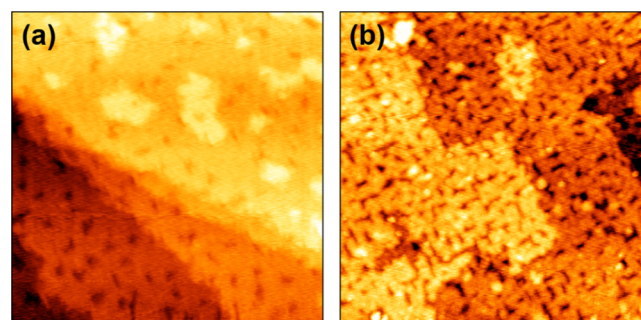


**Figure 5.** STM images ( $150 \text{ nm} \times 150 \text{ nm}$ ) of the two Ga/Cu(001) samples at submonolayer coverages obtained after oxidation in  $10^{-7}$  mbar of  $O_2$  at 700 K. The Ga coverage of the sample shown in (b) is double that of the sample shown in (a). Tunneling parameters: (a) 1.0 V, 0.1 nA and (b) 0.3 V, 0.1 nA.

two oxidized samples at Ga coverages differing by a factor of two. Apparently, depressions (dark spots) in these images correlate with the initial Ga coverage and can be attributed to the Ga oxide phase. Moreover, such spots are elongated and oriented parallel to the two main crystallographic orientations of Cu(001). This finding points to good epitaxial relationships between the  $GaO_x$  layer and the Cu(001) surface underneath. Yet, the atomic resolution of the  $GaO_x$  layer could not be obtained by STM.

Again, we used CO as the probe molecule for the oxidized  $GaO_x$ /Cu(001) surfaces. The TPD spectra measured on two samples of different coverages as well as on pure Cu(001), all exposed to  $1 \times 10^{-7}$  mbar of  $O_2$  at 700 K for 5 min for direct comparison, are shown in Figure 6. (Note that no other



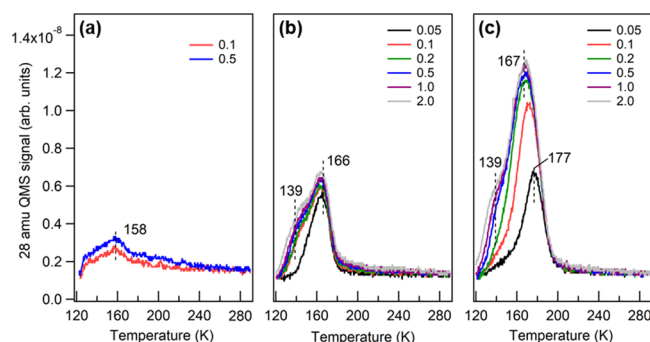


**Figure 6.** CO TPD spectra measured on (a) Cu(100) surface and (b, c) two submonolayer Ga/Cu(100) surfaces, all after annealing in  $1 \times 10^{-7}$  mbar of  $O_2$  at 700 K. The corresponding STM images of the samples shown in (b) and (c) are shown in Figure 5a,b, respectively. CO exposures at 130 K are indicated (in L). The heating rate was 2 K/s. Note that the y-axis scale is by a factor of 5 smaller than in the TPD graphs shown in Figure 2 for the same samples in (a) and (c) before oxidation.

molecules, e.g.,  $CO_2$  and  $H_2O$ , were detected during sample heating to 400 K in these experiments.) The Ga-free Cu(001) sample after oxidation, in essence, does not adsorb CO (Figure 6a), probably due to O adatoms in fourfold hollow sites<sup>21</sup> affecting CO adsorption in the on-top sites.<sup>22</sup> The formation of Ga oxide islands enhances the CO uptake that scales with the Ga coverage (Figure 6b,c), indicating that CO adsorbs primarily on the  $GaO_x$  surface. It is interesting to note that the desorption temperature at CO saturation (167 K) is considerably higher than that on the “as-prepared” bimetallic Ga/Cu(001) surface (153 K, see Figure 2b), although metals typically adsorb CO more strongly than their oxides. On the other hand, the much lower intensities of these signals on both the Ga/Cu(001) and  $GaO_x$ /Cu(001) surfaces as compared to pure Cu(001) (cf Figures 2 and 6) indicate that CO adsorption on the Ga-containing surfaces most likely occurs on low-coordinated sites such as the step edges and corners present in abundance on these surfaces, rather than on the regular terrace sites.

In the next step, we examined the thermal stability of the  $GaO_x$ /Cu(001) surfaces under reducing conditions by exposing the samples to  $10^{-6}$  mbar of  $H_2$  at elevated temperatures, 400–700 K. The XPS results shown in Figure 7 reveal only minor changes. As expected, Cu remains metallic. Some intensity gain of the Cu 2p and Cu LMM signals can be assigned to the removal of the O adatoms as evidenced by the disappearance of the weak O 1s signal at 529.8 eV. Surprisingly, the Ga 2p<sub>3/2</sub> and O 1s signals attributed to the  $GaO_x$  overlayer remain virtually identical in the  $H_2$  atmosphere. A small shift (about 0.3 eV) toward higher binding energies (BEs) observed for the Ga 2p<sub>3/2</sub> state correlates with the disappearance of the 532.3 eV signal in the O1s region and can be assigned to the removal of adventitious impurities on the Ga oxide surface, most likely carbonates, and associated with this charge redistribution.

To study the surface transformations of  $GaO_x$ /Cu(001) films at higher pressures, we used NAP–XPS (Figure 8). However, the spectra measured in 0.18 mbar of pure  $H_2$  at 700 K revealed no features, which would be indicative of the partial Ga oxide reduction, and were, in fact, virtually identical to those measured in  $10^{-6}$  mbar of  $H_2$  (Figure 7). Furthermore, adding  $CO_2$  to  $H_2$  to mimic  $CO_2$  hydrogenation reaction

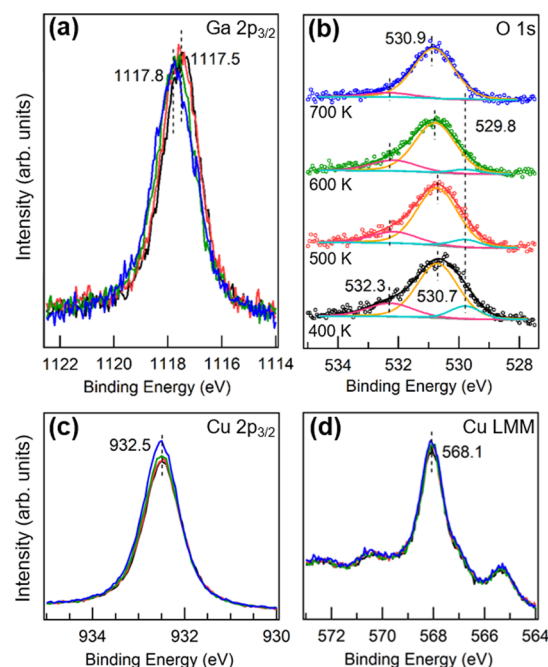


**Figure 7.** XPS spectra measured in UHV at 300 K after annealing the  $GaO_x$ /Cu(001) surface stepwise in  $10^{-6}$  mbar of  $H_2$  at the indicated temperatures. The oxidation of this sample was monitored by XPS and is shown in Figure 4, while the morphology is shown in Figure 3a.

conditions caused no changes in the spectra (Figure 8a–c). Moreover, characterization of this sample with an STM showed the same morphology as before the reactions in the pure  $H_2$  and  $CO_2 + H_2$  mixture. All these findings clearly show that once the Ga oxide layer has been formed, it remains very stable even in a hydrogen-rich atmosphere.

**3.1. General Discussion.** The experimental results presented above may be rationalized as follows. Upon physical vapor deposition of Ga onto Cu(001) at room temperature, Ga adatoms readily intermix within the topmost Cu layer. The surface appears homogeneous, and no preferential Ga adsorption on the step edges or other structural defects is observed. Although the precise mechanism of surface alloying is yet unknown, it probably proceeds via a place-exchange mechanism<sup>23</sup> and/or trapping of the Ga adatoms with the Cu adatoms diffusing on the Cu(001) surface, thus resulting in monolayer-thick islands of a similar composition as the terraces. In principle, Cu and Ga form a stable intermetallic compound at 300 K, namely,  $CuGa_2$ , which in the (001) orientation has a square unit cell like Cu(001). However, the surface lattice constant of  $CuGa_2$ (001) is 2.83 Å, that is, much larger than that of Cu(001) (= 2.55 Å), which could be clearly observed by LEED if really formed. In addition, its formation would cause certain strain due to the substantial lattice mismatch and would be thermodynamically unfavorable.

Oxidation of the resulting bimetallic surface may occur at room temperature even from traces of oxygen in the UHV background, but it accelerates in  $10^{-6}$  mbar of  $O_2$  with increasing annealing temperature and is fully completed at about 500 K. In oxygen ambient, the bimetallic surface undergoes transformation into the Ga oxide phase and the O-covered Cu(001) surface. This phase separation and oxide segregation are clearly observed by STM, where Ga oxide is imaged as rectangular-shaped domains oriented parallel to the main crystallographic directions of the Cu(001) surface. The

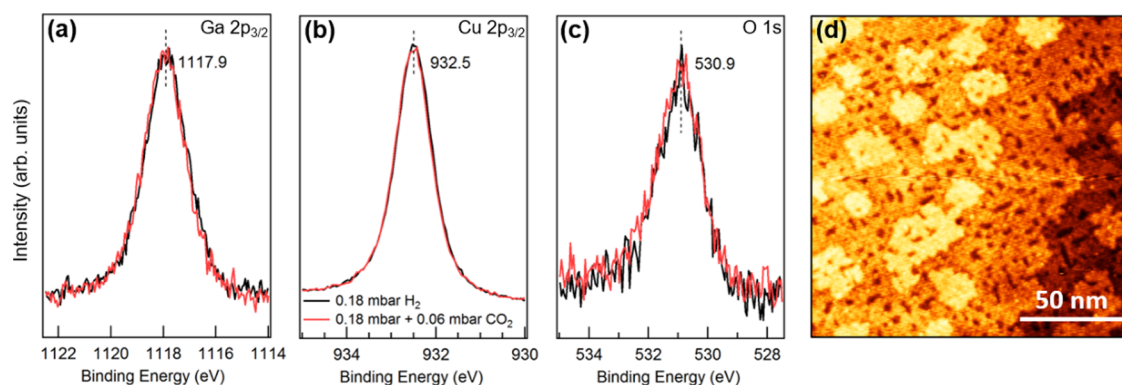


**Figure 8.** (a–c) NAP–XPS spectra measured on a  $\text{GaO}_x/\text{Cu}(001)$  film in 0.18 mbar of  $\text{H}_2$  and in the 0.18 mbar of  $\text{H}_2$  + 0.06 mbar of  $\text{CO}_2$  mixture, both at 700 K. (d) STM image of the sample after the NAP–XPS experiments. Tunneling parameters are bias 1.0 V and current 0.08 nA.

apparent depth of such domains measured by STM is close to or even less than the interlayer distance in Cu, suggesting that electronic effects dominate the image contrast. In addition, one should also consider the model of Ga oxide islands embedded into  $\text{Cu}(001)$  as previously observed, for example, for  $\text{NiO}(001)$  layers on  $\text{Ag}(001)$ .<sup>24</sup> High-resolution STM studies in combination with tunneling spectroscopy would help to validate or discard such a scenario.

The determination of the oxide stoichiometry and the oxidation state of Ga by XPS is not a trivial task in the case of ultrathin oxide films, and this is even more challenging for embedded oxide layers. In addition, the absolute BEs of the Ga core levels reported in the literature for metallic Ga and Ga oxides often deviate. For example, “thick” Ga layers deposited onto a gold foil exhibited a Ga  $2p_{3/2}$  shift to 1117.1 eV and further to 1118.6 eV upon complete oxidation resulting in a stoichiometry close to  $\text{Ga}_2\text{O}_3$ ,<sup>25</sup> whereas ref.<sup>4</sup> reports 1116.4 and 1118.8 eV for Ga and  $\text{Ga}_2\text{O}_3$  samples, respectively. Therefore, the shift caused by oxidation amounts to 1.5 and 2.4 eV in these studies. In our case, the value is 1.1 eV for the oxidized samples (1117.5 vs 1116.4 eV, see Figure 4), which increases to 1.5 eV in hydrogen ambient (Figure 7) presumably due to the removal of surface carbonates. It should be also mentioned that Ga oxide thin films grown by different deposition techniques are commonly assigned to the  $\text{Ga}_2\text{O}_3$  phase,<sup>7</sup> which may, however, exist in several different crystal modifications.

What is most striking is that the Ga oxide phase readily formed in oxygen ambient is extremely stable even at elevated pressures of hydrogen ( $\sim 0.2$  mbar) at 700 K. This finding suggests that once the Ga oxide has been formed, it will remain stable in catalytic hydrogenation reactions, as exemplified here for the  $\text{CO}_2$  hydrogenation conditions. This may also explain the recent results for the Ni–Ga powder catalysts<sup>5</sup> demonstrating that the reduction temperature is critical for the catalytic performance, which can be associated with the presence or absence of the Ga oxide phase.

#### 4. CONCLUSIONS

In this work, we studied the initial stages of the Ga interaction with the  $\text{Cu}(001)$  surface and surface transformations in different gaseous atmospheres in order to get insights into the surface chemistry of the Cu–Ga catalysts recently proposed for  $\text{CO}_2$  hydrogenation to methanol. The results show that Ga readily intermixes with Cu upon deposition in vacuum. However, even traces of oxygen in the gas ambient cause Ga

oxidation and the formation of two-dimensional Ga oxide nanoislands uniformly covering the Cu surface. Such a morphology and the chemical state of Ga remains in pure  $\text{H}_2$  as well as in the  $\text{CO}_2$  +  $\text{H}_2$  reaction mixture. It, therefore, appears that the Ga-promoted Cu surface under reaction conditions exposes a variety of  $\text{GaO}_x/\text{Cu}$  interfacial sites, which may influence the reaction mechanism.

#### ■ ASSOCIATED CONTENT

##### Supporting Information

The Supporting Information is available free of charge at <https://pubs.acs.org/doi/10.1021/acs.jpcc.0c09382>.

Auger spectra of the clean  $\text{Cu}(001)$  and “as-deposited”  $\text{Ga}/\text{Cu}(001)$  surfaces, comparison of the O1s XPS spectra on oxidized  $\text{Cu}(001)$  and  $\text{Ga}/\text{Cu}(001)$  surfaces to differentiate O species, and C1s region in the XPS spectra of the  $\text{Ga}/\text{Cu}(100)$  and  $\text{GaO}_x/\text{Cu}(001)$  surfaces (PDF)

#### ■ AUTHOR INFORMATION

##### Corresponding Author

Shamil Shaikhutdinov – Department of Interface Science, Fritz Haber Institute of the Max Planck Society, Berlin 14195, Germany; [orcid.org/0000-0001-9612-9949](https://orcid.org/0000-0001-9612-9949); Email: [shaikhutdinov@fhi-berlin.mpg.de](mailto:shaikhutdinov@fhi-berlin.mpg.de)

##### Authors

Jian-Qiang Zhong – Department of Interface Science, Fritz Haber Institute of the Max Planck Society, Berlin 14195, Germany; [orcid.org/0000-0003-2351-4381](https://orcid.org/0000-0003-2351-4381)

Beatriz Roldan Cuenya – Department of Interface Science, Fritz Haber Institute of the Max Planck Society, Berlin 14195, Germany; [orcid.org/0000-0002-8025-307X](https://orcid.org/0000-0002-8025-307X)

Complete contact information is available at: <https://pubs.acs.org/doi/10.1021/acs.jpcc.0c09382>

##### Notes

The authors declare no competing financial interest.

#### ■ ACKNOWLEDGMENTS

The work was supported by the European Research Council (Grant ERC-725915, OPERANDOCAT) and the German Research Foundation (DFG) under Germany’s Excellence Strategy—EXC 2008—390540038—“UniSysCat.” J.Q.Z. thanks the AvH Foundation for a postdoctoral fellowship.



## ■ REFERENCES

- (1) Armbrüster, M.; Behrens, M.; Cinquini, F.; Föttinger, K.; Grin, Y.; Haghofer, A.; Klötzer, B.; Knop-Gericke, A.; Lorenz, H.; Ota, A.; et al. How to Control the Selectivity of Palladium-based Catalysts in Hydrogenation Reactions: The Role of Subsurface Chemistry. *ChemCatChem* **2012**, *4*, 1048–1063.
- (2) Studt, F.; Sharafutdinov, I.; Abild-Pedersen, F.; Elkjær, C. F.; Hummelshøj, J. S.; Dahl, S.; Chorkendorff, I.; Nørskov, J. K. Discovery of a Ni-Ga catalyst for carbon dioxide reduction to methanol. *Nat. Chem.* **2014**, *6*, 320.
- (3) Sharafutdinov, I.; Elkjær, C. F.; Pereira de Carvalho, H. W.; Gardini, D.; Chiarello, G. L.; Damsgaard, C. D.; Wagner, J. B.; Grunwaldt, J.-D.; Dahl, S.; Chorkendorff, I. Intermetallic compounds of Ni and Ga as catalysts for the synthesis of methanol. *J. Catal.* **2014**, *320*, 77–88.
- (4) Surdu-Bob, C. C.; Saied, S. O.; Sullivan, J. L. An X-ray photoelectron spectroscopy study of the oxides of GaAs. *Appl. Surf. Sci.* **2001**, *183*, 126–136.
- (5) Gallo, A.; Snider, J. L.; Sokaras, D.; Nordlund, D.; Kroll, T.; Ogasawara, H.; Kovarik, L.; Duyar, M. S.; Jaramillo, T. F. Ni<sub>3</sub>Ga<sub>3</sub> catalysts for CO<sub>2</sub> reduction to methanol: Exploring the role of Ga surface oxidation/reduction on catalytic activity. *Appl. Catal. B: Environ.* **2020**, *267*, 118369.
- (6) Medina, J. C.; Figueroa, M.; Manrique, R.; Rodríguez Pereira, J.; Srinivasan, P. D.; Bravo-Suárez, J. J.; Baldovino Medrano, V. G.; Jiménez, R.; Karelövic, A. Catalytic consequences of Ga promotion on Cu for CO<sub>2</sub> hydrogenation to methanol. *Catal. Sci. Technol.* **2017**, *7*, 3375–3387.
- (7) Pearton, S. J.; Yang, J.; Cary IV, P. H.; Ren, F.; Kim, J.; Tadjer, M. J.; Mastro, M. A. A review of Ga<sub>2</sub>O<sub>3</sub> materials, processing, and devices. *Appl. Phys. Rev.* **2018**, *5*, No. 011301.
- (8) März, A.; Franchy, R. Oxidation of CoGa(110). *Surf. Sci.* **2000**, *466*, 54–65.
- (9) Franchy, R.; Eumann, M.; Schmitz, G. Elemental steps in the growth of thin  $\beta$ -Ga<sub>2</sub>O<sub>3</sub> films on CoGa(100). *Surf. Sci.* **2001**, *470*, 337–346.
- (10) Stierle, A.; Streitel, R.; Nolte, P.; Vlad, A.; Costina, I.; Marsman, M.; Kresse, G.; Lundgren, E.; Andersen, J. N.; Franchy, R.; Dosch, H. Real time observation of ultrathin epitaxial oxide growth during alloy oxidation. *New J. Phys.* **2007**, *9*, 331–331.
- (11) Jeliazova, Y.; Franchy, R. Growth of ultra-thin Ga and Ga<sub>2</sub>O<sub>3</sub> films on Ni(100). *Surf. Sci.* **2003**, *527*, 57–70.
- (12) Jeliazova, Y.; Franchy, R. Vibrational properties of ultrathin Ga<sub>2</sub>O<sub>3</sub> films grown on Ni(100). *Surf. Sci.* **2002**, *502–503*, 51–57.
- (13) Liu, S.; McDonald, S.; Gu, Q.; Matsumura, S.; Qu, D.; Sweatman, K.; Nishimura, T.; Nogita, K. Properties of CuGa<sub>2</sub> Formed Between Liquid Ga and Cu Substrates at Room Temperature. *J. Electron. Mater.* **2020**, *49*, 128–139.
- (14) Li, J. B.; Ji, L. N.; Liang, J. K.; Zhang, Y.; Luo, J.; Li, C. R.; Rao, G. H. A thermodynamic assessment of the copper–gallium system. *Calphad* **2008**, *32*, 447–453.
- (15) Cui, Y.; Liang, F.; Yang, Z.; Xu, S.; Zhao, X.; Ding, Y.; Lin, Z.; Liu, J. Metallic Bond-Enabled Wetting Behavior at the Liquid Ga/CuGa<sub>2</sub> Interfaces. *ACS Appl. Mater. Interfaces* **2018**, *10*, 9203–9210.
- (16) Rodríguez, J. A.; Goodman, D. W. The Nature of the Metal-Metal Bond in Bimetallic Surfaces. *Science* **1992**, *257*, 897.
- (17) Vollmer, S.; Witte, G.; Wöll, C. Determination of Site Specific Adsorption Energies of CO on Copper. *Catal. Lett.* **2001**, *77*, 97–101.
- (18) Liu, B.-H.; Groot, I. M. N.; Pan, Q.; Shaikhutdinov, S.; Freund, H.-J. Ultrathin Zn and ZnO films on Cu(111) as model catalysts. *Appl. Catal. A: Gen.* **2017**, *548*, 16–23.
- (19) Campbell, C. T. Ultrathin metal films and particles on oxide surfaces: structural, electronic and chemisorptive properties. *Surf. Sci. Rep.* **1997**, *27*, 1–3), 1–111.
- (20) Bourque, J. L.; Biesinger, M. C.; Baines, K. M. Chemical state determination of molecular gallium compounds using XPS. *Dalton Trans.* **2016**, *45*, 7678–7696.
- (21) Yagyu, K.; Liu, X.; Yoshimoto, Y.; Nakatsuji, K.; Komori, F. Dissociative Adsorption of Oxygen on Clean Cu(001) Surface. *J. Phys. Chem. C* **2009**, *113*, 5541–5546.
- (22) Gajdoš, M.; Hafner, J. CO adsorption on Cu(111) and Cu(001) surfaces: Improving site preference in DFT calculations. *Surf. Sci.* **2005**, *590*, 117–126.
- (23) Meyer, J. A.; Behm, R. J. Place-exchange as a mechanism for adlayer island nucleation during epitaxial growth and resulting scaling behavior. *Surf. Sci.* **1995**, *322*, L275–L280.
- (24) Steurer, W.; Surnev, S.; Fortunelli, A.; Netzer, F. P. Scanning tunneling microscopy imaging of NiO(100)(1×1) islands embedded in Ag(100). *Surf. Sci.* **2012**, *606*, 803–807.
- (25) Grabau, M.; Steinrück, H.-P.; Papp, C. Physical vapor deposition of Ga on polycrystalline Au surfaces studied using X-ray photoelectron spectroscopy. *Surf. Sci.* **2018**, *677*, 254–257.